Spectrochimica Acta Part A 77 (2010) 579–587

Contents lists available at ScienceDirect

Spectrochimica Acta Part A: Molecular and Biomolecular Spectroscopy

journal homepage: www.elsevier.com/locate/saa

Spectral, thermal and *in vitro* antimicrobial studies of cyclohexylamine-*N*-dithiocarbamate transition metal complexes

Saul M. Mamba[a], Ajay K. Mishra[a,*], Bhekie B. Mamba[a], Patrik B. Njobeh[b], Mike F. Dutton[b], Elvis Fosso-Kankeu[c]

[a] Department of Chemical Technology, University of Johannesburg, PO Box 17011, Johannesburg, Gauteng, Doornfontein 2028, South Africa
[b] Food, Environment and Health Research Group, Faculty of Health Sciences, University of Johannesburg, PO Box 17011, Doornfontein 2028, South Africa
[c] Water and Health Research Unit, Faculty of Health Sciences, University of Johannesburg, PO Box 17011, Doornfontein 2028, Johannesburg, South Africa

ARTICLE INFO

Article history:
Received 8 January 2010
Received in revised form 6 May 2010
Accepted 4 June 2010

Keywords:
Spectral
Thermal
Antimicrobial
DTC
Transition metal
Triphenylphosphine

ABSTRACT

Transition metal complexes of the type $[M(L)_2]$ and those containing monodentate phosphines of the type $[M(L)_2(PPh_3)]$ {M = Ni, Co, Cu and Zn; L = cyclohexylamine-*N*-dithiocarbamate; PPh_3 = triphenylphosphine} have been synthesized. The complexes were characterized using IR, UV–vis, NMR spectroscopy, and thermal analysis (TGA). The ^{1}H NMR, ^{13}C NMR and ^{31}P NMR showed the expected signals for the dithiocarbamate and triphenylphosphine moieties. The spectral studies in all compounds revealed that the coordination of metals occurs *via* the sulphur atom of the dithiocarbamate ligand in a bidentate fashion. Thermal behavior of the complexes showed that the complexes were more stable than their parent ligands. The ligand moiety is lost in the first step and the rest of the organic moiety decomposes in the subsequent steps. Furthermore, the ligand and their metal complexes were screened *in vitro* for their antibacterial activity against *Escherichia coli*, *Staphylococcus aureus*, *Salmonella typhi*, *Enterococcus faecalis*, *Pseudomonas aeruginosa* and *Bacillus cereus* and antifungal activities against *Aspergillus flavus*, *Aspergillus carbonarius*, *Aspergillus niger* and *Aspergillus fumigatus*. The metal complexes exhibited higher antimicrobial activity than the parent ligands. Generally, the zinc complexes were effective against the growth of bacteria with $Zn(L)_2$ displaying broad spectrum bacteriocidal activity at concentrations of 50 μg/mL; and $Ni(L)_2$ was more effective against the growth of fungi at concentrations of 100–400 μg/mL under laboratory conditions.

1. Introduction

Dithiocarbamate-containing coordination compounds are well known and have been widely studied because of their wide biological, industrial, agricultural and chemical applications [1–9]. The dithiocarbamates can be used as nitrogen–oxygen trapping agents [1], chelating agents of heavy metals [2–4], vulcanizers, fungicides, lubricants and catalysts. They have also been used in medicine since the dithiocarbamate moiety has been found in a variety of biologically active molecules [5–9].

Transition metal DTC complexes exhibit both mono- and binuclear types of molecular structure depending on the preparation procedures [10–12]. Nickel(II) complexes of the type $Ni(DTC)_2$ have a mononuclear square planar structure and similar cobalt(II) complexes also exhibit square planar coordination. Copper(II) bis(dithiocarbamate) complexes can be dimeric or monomeric with the monomeric structures adopting the square planar arrangement while dimeric complexes have a five-coordinate geometry around the copper ion [13]. Zinc(II) complexes generally show dimeric non-planar molecular configurations which may be described as distorted tetrahedral, trigonal-bipyramidal or square-pyramidal of the type $Zn_2(DTC)_4$ [14]. Furthermore, zinc(II) complexes can also be monomeric adopting the square planar geometry, which usually depends on the size of the coordinated groups [12–15].

Transition metal derivatives of cyclohexylamine dithiocarbamates have been reported to be promising fungicides [16]. Recently it has been reported that platinum(II) and palladium(II) complexes of substituted cyclohexylamine-*N*-dithiocarbamates displayed low cytotoxicity and antitumor activity [17,18]. However, to the best of our knowledge the biological profiles of the 3-d metal complexes of cyclohexylamine dithiocarbamates have not been studied and reported.

In this paper, we report on the synthesis and characterization of cyclohexylamine-*N*-dithiocarbamate, and mixed-ligand complexes containing triphenylphosphine adducts of nickel(II), cobalt(II), copper(II) and zinc(II). All the complexes were characterized by spectroscopic techniques and thermogravimetric analysis.

* Corresponding author. Tel.: +27 11 559 6180; fax: +27 11 559 6425.
E-mail address: amishra@uj.ac.za (A.K. Mishra).

1386-1425/$ – see front matter © 2010 Elsevier B.V. All rights reserved.
doi:10.1016/j.saa.2010.06.002

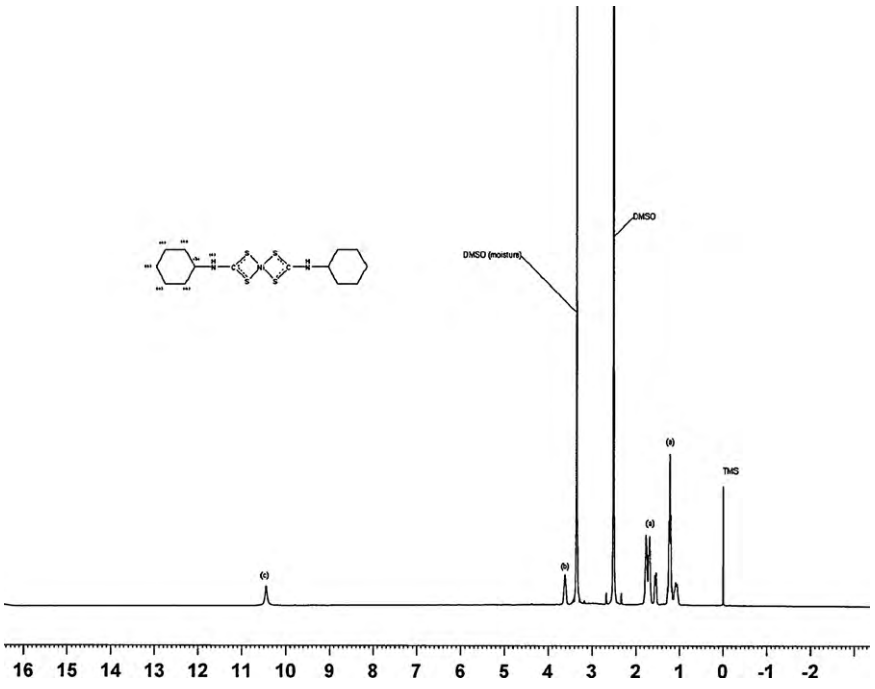

Fig. 1. ^{1}H NMR spectrum of $Ni(L)_2$.

We also report on the antifungal and antibacterial activity of the ligand and selected metal complexes.

2. Experimental

2.1. Materials and reagents

All reagents and solvents used were of the analytical reagents (AR) grade and were used as supplied. The copper(II) chloride dehydrate, cobalt(II) acetate tetrahydrate, nickel(II) acetate tetrahydrate, zinc chloride, potassium hydroxide, carbon disulphide and triphenylphosphine were obtained either from Sigma–Aldrich or from Merck.

2.2. Instruments

IR spectra were recorded on a MIDAC FTIR spectrophotometer in the range 4000–400 cm^{-1} using KBr pellets. The UV–vis spectra were recorded in DMSO on a SHIMADZU 2450 UV-Visible spectrometer. NMR spectra were recorded on a GEMINI-300 MHz spectrophotometer at room temperature using d_6-DMSO as a solvent. ^{13}C NMR spectra were recorded in the proton decoupled mode. Themogravimetric analysis was performed on a PERKIN-ELMER Pyris 1 TG Analyzer under nitrogen atmosphere using alumina pan as a reference. The weight of the sample was between 4 mg and 8 mg and the heating rate was maintained at 10 °C/min from 20 to 900 °C.

2.3. Preparation of cyclohexylamine-N-dithiocarbamate (L)

The ligand was prepared by following a standard method [13]. The potassium salt of the DTC ligand was prepared by nucleophilic addition of carbon disulphide (CS_2) to cyclohexylamine. A methanolic solution of cyclohexylamine (5.7 mL, 50 mmol,) in methanol (15 mL) was added to CS_2 (3.0 mL, 50 mmol) in methanol (10 mL) in the presence of KOH (2.8 g, 0.05 mol) in methanol (20 mL) in a 2 neck round bottom flask. The reaction was maintained at 0–5 °C using a water-ice bath. The resultant yellowish solution was subjected to continuous stirring for 5 h and allowed to evaporate. The yellowish-white solid obtained was then recrystallized in methanol. The product was dried in a vacuum over calcium chloride ($CaCl_2$) overnight (yield: 84%, M.pt.: 72 °C).

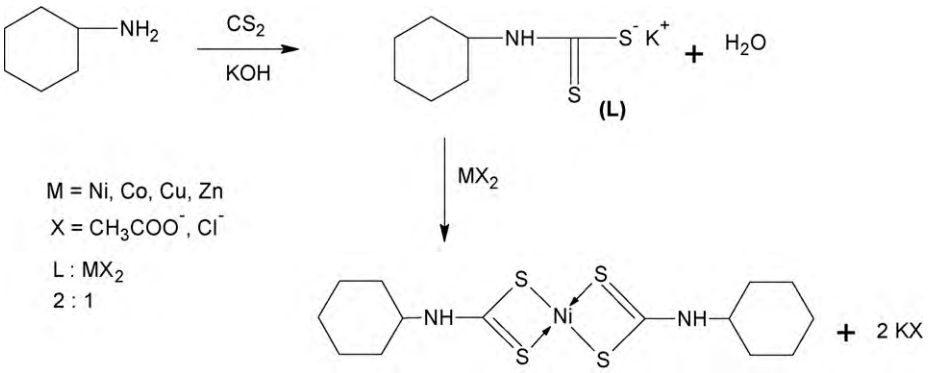

Scheme 1. Preparation of metal complex.

2.4. Preparation of the complexes

2.4.1. Preparation of bis(dithiocarbamato) transition metal complexes

Warm solutions of metal salts (2.5 mmol) {$CuCl_2{\cdot}2H_2O$ (0.43 g), $Co(CH_3COO)_2{\cdot}4H_2O$ (0.62 g), $Ni(CH_3COO)_2{\cdot}4H_2O$ (0.62 g) and $ZnCl_2$ (0.34 g)} in methanol (10 mL) were added drop wise to a solution of L (1.06 g, 5 mmol) in methanol (15 mL). The mixture was then refluxed for 3 h. The precipitates formed were filtered off, washed with water, methanol and petroleum ether. The solids were then dried overnight over $CaCl_2$ under vacuum. Scheme 1 shows a general scheme for accessing the metal complexes.

$Ni(L)_2$: Colour: green, yield: 50%, M.pt.: 160 °C; $Co(L)_2$: colour: dark, yield: 43%, M.pt.: 154 °C; $Cu(L)_2$: Colour: yellow, yield: 66%, M.pt.: charring; $Zn(L)_2$: Colour: white, yield: 54%, M.pt.: 151 °C.

2.4.2. Preparation of phosphine based complexes

A mixture of $Ni(L)_2$ (0.102 g, 0.25 mmol) and PPh_3 (0.066 g, 0.25 mmol) or $Co(L)_2$ (0.204 g, 0.5 mmol) or $Cu(L)_2$ (0.206 g, 0.5 mmol) and PPh_3 (0.13 g, 0.5 mmol) was refluxed in THF (50 mL) for 3 h. The coloured solutions were filtered off and allowed to evaporate without heating. The solids obtained were washed with petroleum ether and dried under vacuum over $CaCl_2$.

Typically, a solution of PPh_3 (0.066 g, 0.25 mmol) in THF (10 mL) was added drop wise to a solution of $Zn(L)_2$ (0.207 g, 0.25 mmol) in THF (50 mL) with stirring. The mixture was refluxed for 3 h and the solvent was evaporated. The white solid obtained was washed with petroleum ether and dried under vacuum over $CaCl_2$.

$[Ni(L)_2PPh_3]$: Colour: green, yield: 69%, M.pt.: 68 °C; $[Co(L)_2PPh_3]$: Colour: dark, yield: 51%, M.pt.: 72 °C; $[Cu(L)_2PPh_3]$: Colour: orange (rusty), yield: 71%, M.pt.: 78 °C; $[Zn(L)_2PPh_3]$: Colour: white, yield: 38%, M.pt.: 75 °C.

2.5. Antimicrobial screening

The antimicrobial activity of the ligand and selected synthesized complexes were tested against some Gram (+) and Gram (−) bacteria and fungi. The activity of the compounds was compared with standard reference drugs.

2.5.1. Antifungal screening

2.5.1.1. Disc diffusion method. A disc application technique was employed *in vitro* to evaluate the antifungal activities of biochemical complexes [19]. Fungi of the *Aspergillus* spp. (*A. flavus*, *A. carbonarius*, *A. niger* and *A. fumigatus*) were used in the study. Mature conidia of fungal isolates were harvested from potato dextrose agar (PDA) plates and suspended in ringer solution and spore suspensions standardized with a haemocytometer (10^4 conidia/mL). Conidial suspension (1 mL) representing each fungal isolate was then spread on a 90-mm petri dish containing PDA (20 mL) with the excess of the conidial suspension decanted and allowed to dry. The compounds were dissolved in dimethyl sulphoxide (DMSO). Sterile 6-mm diameter test discs (AB BioDisk, Solna) were impregnated with 15 μL of the solution of each test compound to contain 100, 200 and 400 μg/disc in triplicates. Amphotericin B (AmB) (20 μg/disc) was used as a reference drug for fungal inhibition, while DMSO was used as a negative control. Plates were incubated at room temperature (22–25 °C) for 7 days. The radius of the inhibition zone of fungal growth on two axes at right angle to each other was measured after 3, 5 and 7 days and expressed as the percentage minimum inhibition zone calculated as follows:

$$\%\ \text{minumun inhibition zone (MIZ)} = \frac{\pi r^2}{\pi R^2} \times 100$$

where $r = r_2 - r_1$; r_2: radius of zone of inhibition of the control (AmB), r_1: radius of zone of inhibition of the test compound and R: radius of petri dish.

Minimum inhibition dose (MID) was defined as the lowest concentration of the tested complex, which showed the least visible fungal growth inhibition.

2.5.1.2. Statistical analysis. A one-way analysis of variance (ANOVA) was performed to derive mean values, which were then compared by least significant difference (LSD) using all pairwise multiple comparison procedures (Holm-Sidak method) (Systat Inc., 2006). Mean values among treatment groups were deemed to have significant differences if the level of probability was ≤ 0.05.

2.5.2. Antibacterial screening

Commercial reference strains of Gram-negative {*Escherichia coli* (*E. coli*), *Pseudomonas aeruginosa* (*P. aeruginosa*) and *Salmonella typhi* (*S. typhi*)} and Gram-positive {*Staphylococcus aureus* (*S. aureus*), *Enterococcus faecalis* (*E. faecalis*) and *Bacillus cereus* (*B. cereus*)} bacteria were selected to assess the potential antibacterial effects of selected ligands and corresponding transition metal complexes.

2.5.2.1. Disc diffusion method. Sterile blank discs (6 mm from Davies Diagnostics (Pty) Ltd., SA) were impregnated with 15 μL of known concentration of stock solution of tested compounds as to obtain discs containing 15, 30, 100, 200 and 400 μg of each compound. Impregnated discs were air-dried and cautiously placed onto the surface of Mueller-Hinton agar (MHA) plates freshly inoculated with microorganisms. After 10 min at room temperature the plated cultures were incubated in an inverted position for 20–24 h at 37 °C.

All microorganisms' culture solutions were adjusted to the turbidity of the 0.5 Mc Farland prior to inoculation onto Mueller-Hinton agar. Experiments were conducted in quadruplicate (four discs with identical concentration of the same compound) and commercial antibiotic (Vancomycin 30 μg and Carbenicillin 100 μg) impregnated discs were used as positive controls. Susceptibility diameter zone was reported as the average value of replicates measurements.

2.5.2.2. Broth dilution method. Stock solution of tested compounds were twofold serially diluted in nutrient broth ("Lab-Lemco" powder: 1.0 g/L; yeast extract 2.0 g/L; peptone 5.0 g/L; sodium chloride 5.0 g/L; pH 7.4 ± 0.2 at 25 °C; Merck Chemicals, SA) contained in sterile test tube to obtain experimental concentrations of 1.53, 3.06, 6.25, 12.5, 25, 50, 100 and 200 μg/mL. Overnight culture (2 mL) of each microorganism was added to the tube, constituting a final concentration of approximately 10^5 CFU/mL in the final volume (4 mL). The mixture was incubated for 18 h at 37 °C. The growth monitored as absorbance at 600 nm using a UV spectrophotometer (Helios Epsilon-USA) and the minimum inhibitory concentration (MIC) determined as the lowest concentration of compound that maintain the turbidity of the solution unchanged through inhibition of growth. The solution in each tube was then inoculated onto nutrient agar plate, and incubated at 37 °C for 24 h to determine the Minimum Bactericidal Concentration (MBC). The highest dilution of a compound that killed >99.9% of the bacteria was considered as the MBC.

3. Results and discussion

The TLC and elemental analysis results (Table 1) revealed that the synthesized ligand and metal complexes were obtained in high purity. The ligand was soluble in most solvents while

Table 1
Elemental analysis.

Compound	Formula	Found (calcd) (%)			
		C	H	N	S
L	$C_7H_{12}KNS_2$	39.05(39.40)	5.80(5.67)	6.89(6.56)	29.95(30.05)
$Ni(L)_2$	$C_{14}H_{24}N_2NiS_4$	41.03(41.28)	5.88(5.94)	6.82(6.88)	31.16(31.94)
$Co(L)_2$	$C_{14}H_{24}CoN_2S_4$	41.36(41.26)	5.82(5.94)	6.82(6.87)	31.95(31.47)
$Cu(L)_2$	$C_{14}H_{24}CuN_2S_4$	40.56(40.80)	5.96(5.87)	6.10(6.80)	30.98(31.12)
$Zn(L)_2$	$C_{14}H_{24}N_2S_4Zn$	40.46(40.61)	5.70(5.84)	6.81(6.77)	30.15(30.98)
$[Ni(L)_2PPh_3]$	$C_{32}H_{39}N_2NiPS_4$	57.02(57.40)	5.77(5.87)	4.25(4.18)	18.99(19.15)
$[Co(L)_2PPh_3]$	$C_{32}H_{39}N_2CoPS_4$	57.45(57.38)	5.83(5.87)	4.11(4.18)	19.06(19.16)
$[Cu(L)_2PPh_3]$	$C_{32}H_{39}N_2CuPS_4$	56.57(56.98)	5.78(5.83)	4.10(4.15)	18.83(19.02)
$[Zn(L)_2PPh_3]$	$C_{32}H_{39}N_2ZnPS_4$	56.23(56.83)	5.82(5.81)	4.67(4.14)	19.02(18.97)

the metal complexes were insoluble in most organic solvents.

3.1. Electronic spectra

The electronic spectral data of the ligand and metal complexes is summarized in Table 2. Dithiocarbamates generally show three bands in the UV region. These bands are ascribed to the intra-molecular intra-ligand transitions corresponding to $\pi \rightarrow \pi^*$ transitions of the N–C=S system, $\pi \rightarrow \pi^*$ transitions of the S–C=S group and a $n \rightarrow \pi^*$ transition located on the sulphur atom [20–22].

The electronic spectra of the ligand showed three electronic bands which were assigned to the $\pi \rightarrow \pi^*$ transitions of the N–C=S system, $\pi \rightarrow \pi^*$ transitions of the S–C=S group and a $n \rightarrow \pi^*$ transition located on the sulphur atom. The electronic spectra of Ni(II) complexes showed two weak d–d bands at 482 and 632 nm. These bands can be assigned to the $^1A_{1g} \rightarrow {}^2B_{2g}$ and $^1A_{1g} \rightarrow {}^1A_{2g}$ transitions [11,12]. This suggests the octahedral geometry for the Ni(II) complex. A band at 382 nm was assigned to metal → ligand charge transfer transitions. The spectrum of the mixed-ligand complex showed an additional band at 412 nm as a result of triphenylphosphine ligand → metal charge transfer transition. Bands below 300 nm were ascribed to $\pi \rightarrow \pi^*$ transitions of the N–C=S and the S–C=S systems.

Two d–d bands were observed in the spectra of cobalt(II) complexes at 642 and 498 nm which were due to the $^4A_{2g}(F) \rightarrow {}^4T_{2g}(F)$ and $^4A_{2g}(F) \rightarrow {}^4T_{1g}(F)$ transitions even though there were three spin allowed transitions [11]. The presence of these bands suggesting the octahedral complexes. Metal → ligand charge transfer (MLCT) transitions were observed at 400 nm and intra-ligand transitions at about 260 and 324 nm.

The copper complexes, $[Cu(L)_2]$ and $[Cu(L)_2PPh_3]$ showed two bands between 250 and 320 nm as a result of intra-ligand and charge transfer transitions, and an unresolved d–d band at nearly 400 nm. These complexes are anticipated as octahedral. For square planar Cu(II) complexes two d–d bands corresponding to $^2B_{1g} \rightarrow {}^2E_g$ and $^2B_{1g} \rightarrow {}^2A_{1g}$ were anticipated while octahedral Cu(II) complexes typically exhibit three unresolved d–d bands assigned to the $^2B_{1g} \rightarrow {}^2B_{2g}$, $^2B_{1g} \rightarrow {}^2E_g$ and $^2B_{1g} \rightarrow {}^2A_{1g}$ transitions [23]. The absence of bands in the region above 900 nm ruled out the possibility of a tetrahedral or pseudo-tetrahedral geometry around the Cu(II) complex [11].

Zinc complexes showed three bands at 260, 278 and 324 nm. The band at 324 nm was assigned to the charge transfer transitions and the other two bands were assigned to $n \rightarrow \pi^*$ and $\pi \rightarrow \pi^*$ transitions. The absorption spectra also showed no d–d bands. There was no chance of transition because there was no empty d-orbital [14,24].

Table 2
Electronic data of the ligand and its metal complexes.

Compound	Wavelength, λ (nm)
L	257, 308
$Ni(L)_2$	252, 327, 381, 482, 632
$Co(L)_2$	269, 323, 400, 550, 658
$Cu(L)_2$	263, 300, 398
$Zn(L)_2$	263, 278, 334
$[Ni(L)_2PPh_3]$	256, 327, 381, 418, 486, 632
$[Co(L)_2PPh_3]$	256, 324, 400, 498, 642
$[Cu(L)_2PPh_3]$	256, 302, 318
$[Zn(L)_2PPh_3]$	260, 278, 324

3.2. Infrared (IR) spectroscopy

Table 3 summarizes the significant IR bands, along with their proposed assignments of the ligand and its complexes. The similarities in the IR spectra of the complexes indicated that they have similar structures. On complexation, the peak at 1482 cm^{-1} attributed to the υ (C.... N) in the ligand was shifted to higher frequency (1500–1522 cm^{-1}) in the complexes. This confirmed an increase in the C–N double bond character due to the mesomeric drift of an electron cloud of the $-NCS_2$ moiety towards the metal ion suggesting a strong contribution of the thioureide resonance form to the structure of dithiocarbamates [11,23]. The υ (C.... S) stretching vibrations are observed at *ca.* 1000 cm^{-1} without any splitting in the complexes suggesting the bidentate coordination of the dithiocarbamate moiety [25]. The presence of only one band in the region 1000 ± 70 cm^{-1} was characteristic of the bidentate nature of the dithiocarbamate ligand. The appearance of two bands within a difference of 20 cm^{-1} in the same region was characteristic of the monodentate binding nature of the ligand [25]. This band was shifted slightly to a higher frequency in the complexes suggesting coordination *via* the C–S group [26].

3.3. NMR spectral studies

Chemical shifts of all the synthesized compounds are summarized below.

Table 3
IR spectral data of L and its complexes.

Compound	Wavenumbers (cm^{-1})		
	υ (N–H)	υ (C.... N)	υ (C.... S)
L	3318	1482	974
$Ni(L)_2$	3235	1513	977
$Co(L)_2$	3245	1500	979
$Cu(L)_2$	3230	1511	977
$Zn(L)_2$	3310, 3249	1513	980
$[Ni(L)_2PPh_3]$	3234	1522	979
$[Co(L)_2PPh_3]$	3267	1501	983
$[Cu(L)_2PPh_3]$	3231	1511	971
$[Zn(L)_2PPh_3]$	3306, 3250	1511	984

3.3.1. ^{1}H NMR spectra

The $-CH_2$ (methylene) protons of all the complexes appeared between 1.00 and 1.95 ppm. The CH–N signal was observed around 4.00 ppm in the ligand and shifted on complexation due to coordination of the ligand to the metal. Fig. 1 shows the NMR spectra of the of $Ni(L)_2$ complex. The deshielding of the protons was attributed to the release of electrons of nitrogen forcing a high electron density towards the sulphur (or metal) *via* the thioureide π-system [27]. Signals between 9 and 11 ppm were assigned to the N–H of the thioureide system [18] and the aromatic protons for the PPh_3 moiety were observed at 7.0–7.8 ppm.

- L, ^{1}H NMR, δ (ppm): 1.00–1.79 (m, 10H, $-CH_2$), 3.72 (s, 1H, –CHN), 9.61 (s, 1H, –NH)
  ^{13}C NMR, δ (ppm): 22.6 (2C), 25.9 (1C), 31.9 (2C), 57.7 (1C, –CHN), 212.6 (1C, $-NCS_2$)
- $Ni(L)_2$, ^{1}H NMR, δ (ppm): 1.1–1.9 (m, 20H, $-CH_2$), 3.8 (brs, 1H, –CHN), 10.4 (brs, 1H, –NH)
  ^{13}C NMR, δ (ppm): 24.2 (4C), 24.6(2C), 31.2(4C), 52.8 (2C), 203.7 (2C)
- $Co(L)_2$, ^{1}H NMR, δ (ppm): 1.11–1.81 (m, 20H, $-CH_2$), 3.74 (brs, 1H, –CHN), 9.99 (brs, 1H, –NH)
  ^{13}C NMR, δ (ppm): 24.1 (4C), 24.6(2C), 31.2(4C), 52.8 (2C), 203.7 (2C)
- $Cu(L)_2$, ^{1}H NMR, δ (ppm): 1.11–1.97 (m, 20H, $-CH_2$), 3.90 (brs, 1H, –CHN), 10.3 (brs, 1H, –NH)
  ^{13}C NMR, δ (ppm): 24.8 (4C), 25.6(2C), 31.2(4C), 52.8 (2C), 203.7 (2C)
- $Zn(L)_2$, ^{1}H NMR, δ (ppm): 1.06–1.83 (m, 20H, $-CH_2$), 3.67 (brs, 1H, –CHN), 9.80 (brs, 1H, –NH)
  ^{13}C NMR, δ (ppm): 24.7 (4C), 25.0(2C), 31.2(4C), 57.5 (2C), 203.7 (2C)
- NiL_2PPh_3, ^{1}H NMR, δ (ppm): 1.02–1.56 (m, 20H, $-CH_2$), 3.4 (brs, 1H, –CHN), 7.0–7.6(m, 15H, Ar), 10.25 (brs, 1H, –NH)
  ^{31}P NMR, δ (ppm): 42.3
- CoL_2PPh_3, ^{1}H NMR, δ (ppm): 1.23–1.85 (m, 20H, $-CH_2$), 3.76 (brs, 1H, –CHN), 7.2–7.7 (m, 15H, Ar), 9.9 (brs, 1H, –NH)
  ^{31}P NMR, δ (ppm): 41.0
- CuL_2PPh_3, ^{1}H NMR, δ (ppm): 1.1–2.1 (m, 20H, $-CH_2$), 3.4 (brs, 1H, –CHN), 7.2–7.8 (m, 15H, Ar), 10.0 (brs, 1H, –NH)
  ^{31}P NMR, δ (ppm): 42.6
- ZnL_2PPh_3, ^{1}H NMR, δ (ppm): 1.22–1.81 (m, 20H, $-CH_2$), 3.4 (brs, 1H, –CHN), 7.12–7.7 (m, 15H, Ar), 9.8 (brs, 1H, –NH)
  ^{31}P NMR, δ (ppm): 43.0

3.3.2. ^{13}C NMR spectroscopy

The $\delta(N^{13}CS_2)$ appeared in the expected region (above 202 ppm) for normal oxidation state transition metal dithiocarbamates [28]. In all metal complexes these signals were observed around 204 ppm. An upfield shift was observed compared to the chemical shift of the parent ligand (at 212 ppm). This upfield shift was caused by the mesomeric shift of the electron density from the dithiocarbamate moiety towards the metal centre [27–29]. The –C–NH carbons of the complexes were observed around 55 ppm and were not greatly affected during complex formation.

3.3.3. ^{31}P NMR spectroscopy

^{31}P NMR was recorded in d_6-DMSO with H_3PO_4 being an internal reference. ^{31}P chemical shifts are observed 42.3, 41.0, 42.6 and 43.0 ppm at for the Ni, Co, Cu and Zn complexes, respectively. The signals are observed in the deshielded region taking into account the free PPh_3 signal at −5.5 ppm. This deshielding effect confirmed the coordination of the phosphorus to the metal and was attributed to the movement of electron density from the phosphorus to the metal atom [29].

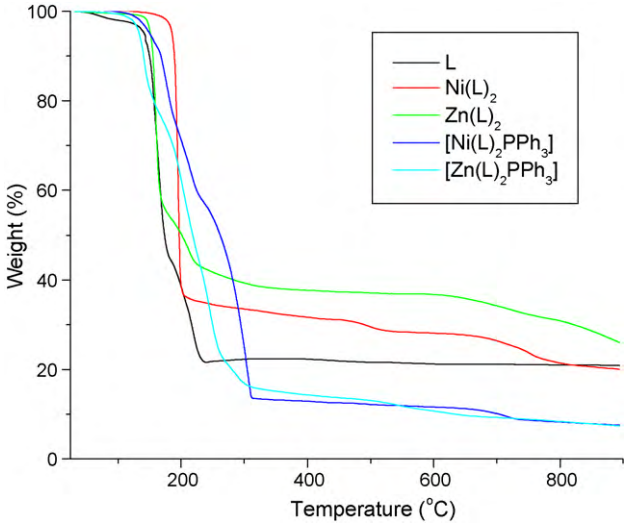

Fig. 2. TG curves of the ligand and selected complexes.

3.4. Thermogravimetric analysis (TGA)

The thermal decomposition of L and its metal complexes is presented in Fig. 2. The ligand, L, decomposed in two steps and it proceeded *via* a potassium thiocyanate intermediate [30]. The first step took place in the range 60–180 °C. Aqueous methanol was lost first at 60–104 °C and this was followed by a sharp decomposition after 104 °C which was assigned to the loss of cyclohexane (found: 53.68, calcd: 54.5%). The decomposition of the intermediate took place in the second step leading to the formation of the final product. $Ni(L)_2$ also decomposed *via* a $Ni(SCN)_2$ intermediate. The first step of the decomposition began at 137 °C and was completed at 208 °C with the loss of 64.0% (calcd: 63.4%). Two cyclohexane molecules and C_2S_2 were eliminated. The decomposition of the intermediate was slow at 211–796 °C. The final product was NiS (found: 20.9%, calcd: 22.3%). The first step in the decomposition of $Zn(L)_2$, from 131 to 346 °C was assigned to the loss of one DTC and one cyclohexane group (found: 61.74%, calcd: 62.3%). The final product was ZnS (found: 26.0%, calcd: 23.2%).

$[Ni(L)_2PPh_3]$ decomposed in three steps. The first step was assigned to the loss of CS_2 (found: 11.2%, calcd: 11.4%). The second step was rapid and total mass loss at this stage was 42.5% (calcd: 42.5%) which matched the loss of two cyclohexane molecules, 2N and a C atom. PPh_3 was lost in the last and final step (found: 79.9%, calcd: 81.6%). The end product of the decomposition was NiS (found: 11.6%, calcd: 13.6%). $[Zn(L)_2PPh_3]$ decomposed in two steps with the first step assigned to the elimination of CS_2 (found: 11.2%, calcd: 11.4%). The elimination of the PPh_3 and the organic moiety occurred in the second and last step. The final product was Zn (found: 7.6%, calcd: 9.6%).

3.5. Antifungal activity

The antifungal activities of the ligand and its corresponding complexes using *Aspergillus* spp. were studied *in vitro* and results are summarized in Tables 4–6. The antifungal activity of the compounds as compared with that of reference drug, AmB showed significant activity. In this case, all compounds tested were active against fungi on Days 3, 6 and 7, with maximum activity observed on $Ni(L)_2$ having an average % MIZ of 4.78 recorded on Day 3. Ni(II) complexes have been found to exhibit maximum biological activity against pathogenic fungi when compared with their parent ligands and similar metal complexes [11,31]. The activity of the metal complexes against the tested fungi was worth noting since

Table 4
Effects of ligand complexes on % MIZ of fungi on Day 3.

Complexes	Conc.	% MIZ			
		A. flavus	*A. carbonarius*	*A. niger*	*A. fumigatus*
L	100	1.53 ± 0.22^{a}	1.81 ± 0.34^{a}	1.71 ± 0.38^{a}	1.36 ± 0.06^{a}
	200	2.66 ± 0.08^{b}	2.53 ± 0.31^{a}	2.85 ± 0.12^{b}	1.49 ± 0.00^{ab}
	400	4.30 ± 0.52^{c}	5.28 ± 0.17^{b}	5.11 ± 0.17^{c}	1.64 ± 0.06^{b}
	Probability	***	***	***	*
$Ni(L)_2$	100	5.31 ± 0.41^{a}	2.41 ± 0.28^{a}	3.92 ± 0.61^{a}	3.05 ± 0.61^{a}
	200	5.40 ± 0.47^{a}	2.84 ± 0.50^{a}	3.96 ± 0.88^{a}	5.28 ± 0.61^{ab}
	400	6.09 ± 1.09^{b}	4.89 ± 1.51^{b}	7.06 ± 0.56^{b}	7.16 ± 0.94^{b}
	Probability	*	**	**	**
$Zn(L)_2$	100	1.01 ± 0.08^{a}	1.47 ± 0.30^{a}	2.44 ± 0.21^{a}	1.82 ± 0.24^{a}
	200	2.54 ± 0.08^{b}	1.66 ± 0.19^{a}	2.56 ± 0.88^{a}	3.70 ± 0.44^{b}
	400	3.01 ± 0.30^{b}	2.27 ± 0.16^{b}	4.13 ± 0.65^{b}	4.47 ± 0.21^{b}
	Probability	***	*	*	***
$[Zn(L)_2PPh_3]$	100	1.12 ± 0.05	0.86 ± 0.04^{a}	1.34 ± 0.25	1.99 ± 0.14^{a}
	200	1.12 ± 0.08	1.00 ± 0.00^{ab}	1.46 ± 0.14	4.87 ± 0.27^{b}
	400	1.29 ± 0.14	1.17 ± 0.10^{b}	1.59 ± 0.06	5.43 ± 0.54^{c}
	Probability	NS	*	NS	***
$[Ni(L)_2PPh_3]$	100	2.04 ± 0.10	1.08 ± 0.05	2.54 ± 0.08^{b}	2.80 ± 0.52^{a}
	200	2.59 ± 0.34	1.28 ± 0.08	2.68 ± 0.26^{a}	3.58 ± 0.19^{ab}
	400	2.39 ± 0.40	1.33 ± 0.08	3.47 ± 0.35^{b}	4.35 ± 0.38^{b}
	Probability	NS	NS	*	*

[a,b,c]Mean values in the same column for each complex not sharing the same letters are significantly different $^{*}p < 0.05$, $^{**}p < 0.01$, $^{***}p < 0.001$. Values within columns are means (left) and standard error of the mean (SEM) (right). NS: not significant; MIZ: minimum inhibitory zone.

Table 5
Effects of ligand complexes on % MIZ of fungi on Day 5.

Complexes	Conc.	% MIZ			
		A. flavus	*A. carbonarius*	*A. niger*	*A. fumigatus*
L	100	0.76 ± 0.06^{a}	0.67 ± 0.06	0.68 ± 0.07	0.88 ± 0.13^{a}
	200	0.86 ± 0.04^{a}	0.83 ± 0.06	0.88 ± 0.12	1.24 ± 0.00^{b}
	400	1.14 ± 0.37^{b}	1.01 ± 0.10	1.06 ± 0.21	1.41 ± 0.05^{b}
	Probability	*	*	NS	***
$Ni(L)_2$	100	1.83 ± 0.04	1.50 ± 0.06^{a}	1.26 ± 0.17	1.02 ± 0.11^{a}
	200	1.91 ± 0.00	1.59 ± 0.00^{a}	1.46 ± 0.08	1.17 ± 0.07^{a}
	400	1.98 ± 0.00	1.83 ± 0.04^{b}	1.57 ± 0.09	1.24 ± 0.06^{b}
	Probability	NS	**	NS	*
$Zn(L)_2$	100	0.61 ± 0.00^{a}	0.64 ± 0.07^{a}	0.79 ± 0.00^{a}	0.44 ± 0.00^{a}
	200	0.61 ± 0.00^{a}	0.70 ± 0.07^{b}	0.86 ± 0.04^{a}	0.79 ± 0.00^{b}
	400	0.79 ± 0.00^{b}	0.90 ± 0.05^{b}	1.17 ± 0.10^{b}	0.90 ± 0.05^{c}
	Probability	*	*	**	**
$[Zn(L)_2PPh_3]$	100	0.68 ± 0.07	0.68 ± 0.07	0.82 ± 0.15	0.79 ± 0.00
	200	0.68 ± 0.07	0.68 ± 0.07	0.88 ± 0.13	0.79 ± 0.00
	400	0.79 ± 0.00	0.79 ± 0.00	1.25 ± 0.11	0.79 ± 0.00
	Probability	NS	NS	NS	NS
$[Ni(L)_2PPh_3]$	100	0.79 ± 0.00	0.88 ± 0.12	0.79 ± 0.00^{a}	0.55 ± 0.03^{a}
	200	0.94 ± 0.09	0.88 ± 0.12	1.03 ± 0.17^{ab}	0.67 ± 0.04^{b}
	400	0.94 ± 0.11	1.03 ± 0.05	1.41 ± 0.05^{b}	0.79 ± 0.00^{c}
	Probability	NS	NS	*	***

[a,b,c]Mean values in the same column for each complex not sharing the same letters are significantly different $^{*}p < 0.05$, $^{**}p < 0.01$, $^{***}p < 0.001$, NS: not significant. Values within columns are means (left) and standard error of the mean (SEM) (right). MIZ: minimum inhibitory zone.

such activity may either be associated with cell wall destruction [31], DNA damage [32], protein synthesis inhibition or chelation with metal ions in fungal cells thus depriving them of the needed ions which would lead to cell mortality [11,33]. Data obtained also indicate that with increasing dosage level of $Ni(L)_2$ from 100 to 400 μg/disc, % MIZ significantly ($p < 0.01$) increased by approximately twofolds, except for *A. flavus* (5.31–6.09%) (Table 4) while % MIZ slightly increased from 5.31 to 6.09 ($p < 0.05$). Although L_2 was less active than $Ni(L)_2$, its activity increased threefolds with dose increment ($p < 0.001$), except in the case of *A. fumigatus* whose MIZ also marginally increased from 1.36 to 1.64%.

Generally, the results obtained suggested that while some complexes tested were less active against *A. carbonarius*, have higher activities on the growth of *A. flavus*, *A. niger* and *A. fumigates*. L showed maximum activity against *A. carbonarius* with low activity exhibited against the growth of *A. fumigatus*.

The compounds reported herein exhibited antifungal activity against fungi after Day 5 (Tables 5 and 6). Such inhibitory data provided by the tested compounds should be considered they are effective, especially when such activity is comparable with that of AmB. More importantly in this context, was the broad spectrum activity exhibited by the tested compounds in inhibiting the growth of more than one fungus. In most situations, biological activities of compounds are often evaluated after 2 days [31] or 4 days [11,34], but in this case, the long lasting efficacy of these compounds was determined up till the seventh day, which still

Table 6
Effects of ligand complexes on % MIZ of fungi on Day 7.

Complexes	Conc.	% MIZ			
		A. flavus	*A. carbonarius*	*A. niger*	*A. fumigatus*
L	100	0.86 ± 0.04^{a}	0.64 ± 0.03^{a}	0.44 ± 0.00^{a}	0.73 ± 0.06
	200	0.93 ± 0.04^{a}	1.21 ± 0.49^{a}	0.64 ± 0.07^{ab}	0.75 ± 0.12
	400	1.08 ± 0.05^{b}	1.45 ± 0.53^{b}	0.73 ± 0.04^{b}	0.80 ± 0.09
	Probability	**	NS	**	NS
$Ni(L)_2$	100	0.96 ± 0.15	0.94 ± 0.09^{a}	1.09 ± 0.09	0.98 ± 0.11^{a}
	200	1.12 ± 0.08	1.24 ± 0.09^{b}	1.09 ± 0.09	1.24 ± 0.00^{ab}
	400	1.08 ± 0.05	1.28 ± 0.04^{b}	1.24 ± 0.00	1.42 ± 0.12^{b}
	Probability	NS	*	NS	**
$Zn(L)_2$	100	0.44 ± 0.00^{a}	0.61 ± 0.06^{a}	0.87 ± 0.08	0.44 ± 0.00^{a}
	200	0.44 ± 0.00^{a}	0.67 ± 0.04^{a}	0.79 ± 0.05	0.61 ± 0.00^{b}
	400	0.79 ± 0.00^{b}	0.86 ± 0.04^{b}	0.80 ± 0.09	0.68 ± 0.07^{b}
	Probability	**	**	NS	*
$[Zn(L)_2PPh_3]$	100	0.44 ± 0.00^{a}	0.61 ± 0.10	0.88 ± 0.12	0.85 ± 0.13^{a}
	200	0.73 ± 0.04^{b}	0.68 ± 0.03	0.94 ± 0.18	1.04 ± 0.07^{a}
	400	0.79 ± 0.00^{b}	0.70 ± 0.04	1.08 ± 0.05	1.33 ± 0.10^{b}
	Probability	**	NS	NS	*
$[Ni(L)_2PPh_3]$	100	0.68 ± 0.07^{a}	0.86 ± 0.04^{a}	0.67 ± 0.04^{a}	0.75 ± 0.12
	200	0.94 ± 0.09^{ab}	0.89 ± 0.00^{a}	1.09 ± 0.09^{a}	0.82 ± 0.15
	400	1.17 ± 0.13^{b}	1.00 ± 0.00^{b}	2.65 ± 0.70^{b}	0.94 ± 0.09
	Probability	*	***	*	NS

[a,b,c]Mean values in the same column for each complex not sharing the same letters are significantly different $^{*}p < 0.05$, $^{**}p < 0.01$, $^{***}p < 0.001$, NS: not significant. Values within columns are means (left) and standard error of the mean (SEM) (right). MIZ: minimum inhibitory zone.

Table 7
Determination of antibacterial activity by disc diffusion.

Selected bacteria	Carbenicillin 100 μg	Vancomycin 30 μg	L	$Ni(L)_2$	$Co(L)_2$	$Zn(L)_2$	$[Cu(L)_2PPh_3]$	$[Zn(L)_2PPh_3]$	Disc content (μg/disc)
			Inhibitory activity						
Escherichia coli	+	+	–	–	–	+	–	+	15
			–	–	–	+	–	+	30
			+	–	–	+	–	+	100
			+	–	–	+	–	+	200
			+	–	–	+	–	+	400
Pseudomonas aeruginosa	+	–	–	+	–	–	+	–	15
			–	+	–	–	+	–	30
			–	+	+	–	+	–	100
			–	+	+	–	+	–	200
			–	+	+	–	+	–	400
Salmonella typhi	+	–	–	–	–	–	–	–	15
			–	–	–	–	–	–	30
			–	–	–	+	–	+	100
			+	–	–	+	–	+	200
			+	–	–	+	–	+	400
Staphylococcus aureus	+	+	–	+	–	+	–	–	15
			–	+	–	+	–	–	30
			+	+	–	+	–	+	100
			+	+	–	+	–	+	200
			+	+	–	+	–	+	400
Enterococcus faecalis	+	+	–	–	–	–	–	–	15
			–	–	–	–	–	–	30
			–	–	–	+	–	–	100
			–	–	–	+	–	–	200
			–	–	–	+	–	–	400
Bacillus cereus	+	+	–	–	–	–	–	–	15
			–	–	–	+	–	+	30
			+	–	–	+	–	+	100
			+	–	–	+	–	+	200
			+	–	–	+	–	+	400

(–): resistant; (+): susceptible.

showed some activity. The decrease in biological activity of these compounds over time might be attributed to the reduced stability of such compounds, especially under neutral and acidic conditions [35]. Alternatively, the reduced activity of compounds with time could be that, there is likely a tendency for some fungi to reduce sensitivity and develop resistance over time by adapting to such applications [36].

When making a choice between various therapeutic applications, the chosen antifungal drug among other factors, must have a long lasting potential. In this study, the prolonged effect of

Table 8
MIC and MBC values of tested compounds.

Selected bacteria	L	$Ni(L)_2$	$Co(L)_2$	$Zn(L)_2$	$[Cu(L)_2PPh_3]$	$[Zn(L)_2PPh_3]$
	MIC(MBC) (μg/mL)					
Escherichia coli	100–100	200–nf	nf–nf	100–50	nf–100	nf–nf
Pseudomonas aeruginosa	100–200	nf–200	nf–200	100–100	nf–100	100–100
Salmonella typhi	100–200	nf–nf	200–nf	50–50	nf–200	nf–100
Staphylococcus aureus	100–200	nf–nf	200–nf	50–50	nf–200	200–200
Enterococcus faecalis	100–nf	200–nf	200–nf	100–200	nf–200	nf–nf
Bacillus cereus	100–100	200–200	nf–nf	100–50	nf–50	100–100

compounds against fungal growth typically in the case of nickel complexes as earlier indicated as well as their broad spectrum activity, was noted. It is, therefore, necessary to evaluate the cytotoxic effects of these compounds as their applications in the formulation of novel antifungal therapeutic drugs seem promising.

3.6. Antibacterial studies

3.6.1. Bacterial susceptibility to tested compounds

The disc diffusion assay was conducted to determine if the tested compounds could inhibit the growth of bacteria. The results obtained revealed inhibitory activity of all tested compounds against at least one microorganism (Table 7) and the inhibition concentration ranged from 15 to 400 μg/disc. $Zn(L)_2$ generally exhibited strong inhibitory activity than any other compound. The compounds inhibitory activity was greater against *S. aureus*, while *E. faecalis* was resistant to most of the complexes and compounds tested.

3.6.2. Minimum inhibitory and Minimum Bactericidal Concentration

Microorganisms are developing resistance against some of the antibacterial compounds available on the market. Candidate compounds for substitution of existing one, should exhibit strong inhibitory activity at very low concentration. The effectiveness of tested compounds in this study was then assessed through determination of MIC and MBC. Results recorded revealed that among all the compounds $Zn(L)_2$ was effective at lower concentration (50 μg/mL) and also exhibit bactericidal activity against all the bacteria (Table 8).

On the other hand $Co(L)_2$ was the compound with the weakest activity against bacteria and mostly static except with *P. aeruginosa*. Although $[Cu(L)_2PPh_3]$ exhibited bactericidal activity against all bacteria, it was not possible to determine the MIC from its activity up to a concentration of 200 μg/mL. This implies that inhibitory activity of $[Cu(L)_2PPh_3]$ against bacteria was very slow and did not prevent the growth from the first hours of incubation, hence the increase of turbidity observed in the tube; copper is a bio-essential element which acts as cofactor for many enzymes [37]. The inhibitory effect of copper results from DNA damage due to the ease of reduction of Cu(II) to Cu(I) [38,39]. However the inhibitory activity of complexes is the summation of the effects of the ligand and the metal which affect both the bacterial cell wall and metabolism [39,40].

4. Conclusions

The characterization techniques confirm that both dithiocarbamate ligands are bidentately coordinated to the metal atom *via* the sulphur atoms. The metal complexes exhibit antibacterial activity against the chosen bacterial species. The zinc dithiocarbamate complex exhibited antibacterial activity against five bacterial species. Broad spectrum bactericidal activity is displayed by the triphenylphosphine adduct of the copper complex. The complexes also show broad antifungal activity and maximum activity being exhibited by the nickel(II) complex. Because of the broad spectrum activity displayed by some of the tested compounds, it is would be necessary to evaluate the cytotoxicity of these compounds as their applications in the formulation of novel antimicrobial therapeutic drugs seem promising.

Acknowledgements

The authors are thankful to the National Research Foundation (NRF) and Nanotech Innovation Centre (NIC) for financially supporting this work.

References

[1] K.S. Siqqidi, S.A.A. Nami, L. Chebude, Y. Chebude, Journal of Brazilian Chemical Society 17 (1) (2006) 107–112.
[2] R. Say, E. Birlik, Z. Erdemgil, A. Denizli, A. Ersoz, Journal of Hazardous Materials 150 (2008) 560–564.
[3] N. Unlu, M. Ersoz, Separation and Purification Technology 52 (2007) 461–469.
[4] F. Fu, H. Zeng, Q. Cai, R. Qiu, J. Yu, Y. Xiong, Chemosphere 69 (2007) 1783–1789.
[5] Y. Yoshikawa, Y. Adachi, H. Sukurai, Life Sciences 80 (2007) 759–766.
[6] S. Ozkirimli, T.I. Apak, M. Kiraz, Yegenoglu, Archives of Pharmacal Research 28 (11) (2005) 1213–1218.
[7] F. Shaheen, A. Badshah, M. Gielen, C. Gieck, M. Jamil, D. de Vos, Journal of Organometallic Chemistry 693 (2008) 1117–1126.
[8] V. Alverdi, L. Giovagnini, C. Marzamo, R. Seraglia, F. Bettio, S. Sitran, R. Graziani, D. Fregona, Journal of Inorganic Biochemistry 98 (2004) 1117–1128.
[9] R. Singh, N.K. Kaushik, Spectrochimica Acta Part A 71 (2) (2008) 669–675.
[10] H.D. Yin, J. Zhai, Y.Y. Sun, D.Q. Wang, Polyhedron 27 (2008) 663–670.
[11] A. Mohammad, C. Varshney, S.A.A. Nami, Spectrochimica Acta Part A 73 (2009) 20–24.
[12] K.D. Karlin, Progress in Inorganic Chemistry, vol. 53, John Wiley and Sons, Inc., New Jersey, 2005, p. 71.
[13] D. Chen, L. Powers, Journal of Inorganic Biochemistry 58 (1995) 245–253.
[14] A.V. Ivanov, T. Rodyna, O.N. Antzutkin, Polyhedron 17 (18) (1998) 3101–3109.
[15] Y. Yang, B. Zuo, J. Li, G. Chen, Spectrochimica Acta Part A 52 (1996) 1915–1919.
[16] T.S. Carswell, H.L. Morill, Industrial and Engineering Chemistry (1937) 1247–1251.
[17] N. Manav, A.K. Mishra, N.K. Kaushik, Spectrochimica Acta Part A 65 (2006) 32–35.
[18] N. Manav, A.K. Mishra, N.K. Kaushik, Spectrochimica Acta Part A 60 (2004) 3087–3092.
[19] A.P. Rauter, Lucas, T. Almeida, D. Sacoto, V. Ribeiro, J. Justino, A. Neves, F.V.M. Silva, M.C. Oliveira, M.J. Ferreira, M.S. Santosa, E. Barbosaa, Carbohydrate Research 340 (2005) 191–201.
[20] M.R.L. Oliviera, V.M. de Bellis, Transition Metal Chemistry 24 (1999) 127–130.
[21] A. Vandebeek, S.J. Joris, K.I. Aspila, C.L. Chakrabarti, Canadian Journal of Chemistry 48 (1970) 2204–2209.
[22] N. Geetha, S. Thirumaran, Journal of the Serbian Chemical Society 73 (2) (2008) 169–177.
[23] K.S. Siddiqi, S. Khan, S.A.A. Nami, M.M. El-ajaily, Spectrochimica Acta Part A. 67 (2007) 995–1002.
[24] R.M. Desai, M.K. Shah, V.H. Shah, E-Journal of Chemistry 3 (12) (2006) 137–141.
[25] S.A.A. Nami, K.S. Siddiqi, Synthesis and Reactivity in Inorganic, Metal-Organic and Nanometal Chemistry 34 (9) (2005) 1581–1590.
[26] G.G. Mohamed, A.N. Ibrahim, A.E.H. Attia, Spectrochimica Acta Part A 72 (2009) 610–615.
[27] A.B. Prakasam, K. Ramalingam, G. Boceli, A. Cantoni, Polyhedron 26 (2007) 4489–4493.
[28] H.L.M. Van Gaal, J.W. Diesveld, F.W. Pijpers, J.G.M. Van der Linden, Inorganic Chemistry 18 (11) (1979) 3251–3260.
[29] A.B. Prakasam, K. Ramalingam, G. Boceli, A. Cantoni, Polyhedron 26 (2007) 1133–1138.
[30] V.T. Yilmaz, T.K. Yazicilar, H. Cesur, R. Ozkanca, F.Z. Maras, Synthesis and Reactivity in Inorganic, Metal-Organic and Nanometal Chemistry 33 (4) (2003) 589–605.

[31] A.K. Mishra, N.K. Kaushik, Spectrochimica Acta Part A 69 (2008) 842–848.
[32] C. Pellerito, L. Nagy, L. Pellerito, A. Szorcsik, Journal of Organometallic Chemistry 691 (2006) 1733–1747.
[33] H. van den Bossche, F. Dromer, L. Improvissi, M. Lozane-Chiu, J.H. Hex, D. Sanglard, Medical Mycology 36 (1998) 119–128.
[34] N.V. Loginova, T.V. Koval'chuk, G.I. Polozov, N.P. Osipovich, P.G. Rytik, I.I. Kucherov, A.A. Chernyavskaya, V.L. Sorokin, O.I. Shadyro, European Journal of Medicinal Chemistry 43 (2008) 1536–1542.
[35] I. Rogachev, V. Gusis, A. Gusis, J.L. Cortina, J. Gressel, A. Warshawsky, Reactive and Functional Polymers 42 (1999) 243–254.
[36] M.B. Klix, J.A. Verreet, M. Beyer, Crop Protection 26 (2007) 683–690.
[37] L.Z. Li, C.T. Zhao, T. Xu, H.W. Ji, Y.H. Yu, G.Q. Guo, H. Chao, Journal of Inorganic Biochemistry 99 (2005) 1076–1082.
[38] K.R. Rupesh, S. Deepalatha, M. Krishnaveni, Venkatesan, S. Jayachandran, European Journal of Medicinal Chemistry 41 (2006) 1494–1503.
[39] S. Khan, S.A.A. Nami, K.S. Siddiqi, E. Husain, I. Naseem, Spectrochimica Acta Part A: Molecular and Biomolecular Spectroscopy 72 (2009) 421–428.
[40] J.G. Cappuccino, N. Sherman, Microbiology—A Laboratory Manual, 6th ed., Pearson Education, San Francisco, USA, 2002, p. 263.